Detection of Blood Vessels in Retinal Images Using Two-Dimensional Matched Filters

SUBHASIS CHAUDHURI, STUDENT MEMBER, IEEE, SHANKAR CHATTERJEE, MEMBER, IEEE, NORMAN KATZ, MARK NELSON, AND MICHAEL GOLDBAUM

Abstract—**Although current literature abounds in a variety of edge detection algorithms, they do not always lead to acceptable results in extracting various features in an image. In this paper, we address the problem of detecting blood vessels in retinal images. Blood vessels usually have poor local contrast and the application of existing edge detection algorithms yield results which are not satisfactory. We introduce an operator for feature extraction based on the optical and spatial properties of objects to be recognized. The gray-level profile of the cross section of a blood vessel is approximated by a Gaussian shaped curve. The concept of matched filter detection of signals is used to detect piecewise linear segments of blood vessels in these images. We construct 12 different templates that are used to search for vessel segments along all possible directions. We discuss various issues related to the implementation of these matched filters. The results are compared to those obtained with other methods. The automatic detection of blood vessels in the retina could help physicians in diagnosing ocular diseases.**

I. INTRODUCTION

EDGE detection plays an important role in a number of image processing applications such as scene analysis and object recognition. The edges in an image provide useful structural information about object boundaries, as the edges are caused by changes in some physical properties of surfaces being photographed, such as illumination, geometry, and reflectance. An edge is, therefore, defined as a local change or discontinuity in image luminance.

There are two basic approaches to edge detection: the enhancement/thresholding method and the edge fitting method [1]. In the former method, the discontinuities in the image gray tone are enhanced by neighborhood operators. The simplest type of differential operator, the Robert's operator, was introduced more than two decades ago. This operator consists of 2×2 convolutional kernels. Prewitt and Sobel operators [2] are improvements on Robert's operator, where the masks have sizes 3×3 pixels. A quantitative comparison of the performances of these operators have been reported in [1]. All of these operators yield good results when the edges are sharp. The presence of noise in the image degrades the performance of gradient based algorithms appreciably. The use of gray-scale morphology has been suggested in [3]. It involves simple erosion and dilation operators and can be implemented for real time processing by using suitable hardware. This algorithm appears to work better in extracting edges from images with salt-and-pepper type of noise.

The Sobel operator involves the computation of local intensity gradients and the responses due to nonideal step edges are not good. A modification of that is the detection of second-order zero-crossings, and the corresponding edge operator is called the Laplacian [2]. In order to reduce the effect of high frequency noise, a bandwidth restriction can be imposed by convolving the original data by a two-dimensional Gaussian window before applying the Laplacian operator [4]–[7]. It has been shown in [4] that the above scheme is a limiting process of the difference of Gaussian (DOG) filter. The advantage of using a Gaussian filter is that it regularizes the ill-posed problem of differentiation [8].

Algorithms belonging to the second category, the edge fitting method, minimize the distance between the original noisy data and a predefined edge model in a finite-dimensional space. Thus, the results of these algorithms are optimal for the chosen edge model and are less sensitive to noise. However, they usually involve more computations. One such algorithm that recognizes edges and lines (edges of finite thickness) was introduced by Hueckel [9], [10]. Here both the edge template and the picture function (within the specified window) are parameterized and are represented by corresponding vectors of coefficients. The Euclidean distance between these two vectors is minimized. Although this algorithm performs very well, a significant savings in computation can be achieved by using the scheme proposed in [11]. Hueckel used the Fourier series in polar coordinates as basis functions to obtain the orthogonal components. These basis functions are replaced by a seemingly reasonable choice of Walsh functions which do not require any floating point multiplications or divisions. Attempts have also been made to detect object boundaries by projecting the data onto a complete set of basis functions in a Hilbert space, which are mutually orthogonal [12]. An optimal frequency domain filter for edge detection has been suggested in [13], where the filter transfer function is specified in terms of prolate

Manuscript received September 12, 1988; revised March 31, 1989. This work was supported by the United States Public Health Service under Research Grant EY 05996-02.

S. Chaudhuri and S. Chatterjee are with the Department of Electrical Engineering, University of California, San Diego, La Jolla, CA 92093.

N. Katz, M. Nelson, and M. Goldbaum are with the Department of Opthalmology, University of California, San Diego, La Jolla, CA 92093.

IEEE Log Number 8928436.

spheroidal wave functions. This filter is optimal in the sense that it produces maximum energy for a specified resolution of edge localization in the vicinity of the edge. A stochastic model of the edge structure in the image has been proposed in [14], where a two-dimensional digital recursive filter has been used to minimize the least mean square (LMS) estimation errors. Characterization of individual edge elements in an image by using generalized splines and discrete cosine transform (DCT), in relation to its neighborhood and in terms of the topographic properties of the image intensity surface, has been reported in [15].

An important motivation for using algorithms based on template matching is the ease of implementation on specialized high speed hardware as well as the possibility for parallel computations. In all of these approaches, computations could be performed in parallel on individual pixels. Such kernel-based methods for edge detection have, thus, become increasingly popular. As the size of the convolution mask is increased, a better operator (in the sense that it is less sensitive to noise) can be designed, but the computation increases significantly. Although these methods may reduce the spatial resolution significantly [11], they may be used very efficiently not just to detect individual edge elements but to extract certain special features in the image. Our goal is to design an operator which is nearly optimal for the recognition of certain special objects in the image, particularly for the detection of blood vessels in retinal fundus images.

The organization of this paper is as follows. The importance of edge detection in image processing applications and the currently available different types of edge detectors have been reviewed in this section. Section II describes the need for the detection of blood vessels in retinal images and a brief survey of the existing literature. Some of the special properties of blood vessels in fundus images are reported in Section III. The concept of matched filter detection of signals is briefly reviewed here, and then extended to the detection problem for 2-D signals. Section IV describes the implementation of the proposed algorithm. Some of the results of application of this scheme to fundus images are given in Section V. The performance of this algorithm is compared to that of some other commonly known algorithms. Finally, conclusions and recommendations are presented in Section VI.

II. Detection of Blood Vessels

Information about blood vessels can be used in grading disease severity or as part of the process of automated diagnosis of diseases with ocular manifestations [16]–[18]. Blood vessels can act as landmarks for localizing the optic nerve, the fovea (central vision area), and lesions. As a result of systemic or local ocular disease, the blood vessels can have measurable abnormalities in diameter, color, and tortuosity. For example, central retinal artery occlusion usually causes generalized constriction of retinal arteries, hypertension may result in focal constriction of retinal arteries, central retinal vein occlusion typically produces dilated tortuous veins, arteriosclerosis can cause the arteries to acquire a copper or silver color, and diabetes can generate new blood vessels (neovascularization). Thus, a reliable method of vessel detection is needed, which preserves various vessel measurements.

An edge detection algorithm, similar to the morphological edge detector, has been used for automatic recognition of arterio-venous intersections [19]. A line finding algorithm along with a probabilistic relaxation scheme has been used for the extraction and subsequent description of blood vessel patterns in retinal images [20], [21]. However, these algorithms do not result in a continuous map of the vasculature of the retinal surface. An individual blood vessel may be broken into several segments due to branching of vessels or arteriovenous intersections.

Most of the algorithms mentioned above and in the previous section may be considered as generalized edge detectors, and do not take account of the special properties of the objects being detected. Blood vessels have a special property that the two edges of a vessel always run parallel to each other. Such objects may be represented by piecewise linear directed segments of finite width. The gradient directions for these two edge elements are 180° apart and hence, they are sometimes referred to as "anti-parallels" [22]. Thus, one method of extraction of such objects in an image consists of identifying the anti-parallels and tracking them along their gradient directions [22]. This algorithm has been used for locating roads, rivers, etc., in geological images. In our experience, the contrast between vessels and the background was too low for these methods to reliably define blood vessels without fragmentation [23].

Methods of extraction or enhancement of directed line segments in an image have been proposed in [24], [25]. These methods employ sector filters in the frequency domain and fail to yield good results in the presence of blob type objects in the image [26]. It has recently been brought to our attention that a method of enhancement of fingerprints has been proposed in [27], [28]. The intensity profiles for individual lines are modeled by cosine shaped curves, the dominant angle of orientation in a local neighborhood is estimated, and then a proper template is used to enhance the line segments. However, the process of estimating the local orientation consumes about 85 percent of the computation time. The method that we propose here is quite similar to the above approach, but it does not require this pre-processing step. The proposed method is discussed in the next section.

III. Design of Matched Filter

We observe three interesting properties of the blood vessels in retinal images.

1) Since the blood vessels usually have small curvatures, the anti-parallel pairs may be approximated by piecewise linear segments.

2) Since the vessels have lower reflectance compared to other retinal surfaces, they appear darker relative to the background. A few representative samples of blood vessel

gray-level profiles along directions perpendicular to their length are plotted in Fig. 1. It was observed that these vessels almost never have ideal step edges. Although the intensity profile varies by a small amount from vessel to vessel, it may be approximated by a Gaussian curve $f(x, y) = A\{1 - k \exp(-d^2/2\sigma^2)\}$, where d is the perpendicular distance between the point (x, y) and the straight line passing through the center of the blood vessel in a direction along its length, σ defines the spread of the intensity profile, A is the gray-level intensity of the local background, and k is a measure of reflectance of the blood vessel relative to its neighborhood.

3) Although the width of a vessel decreases as it travels radially outward from the optic disk, such a change in vessel caliber is a gradual one. The widths of the vessels are found to lie within a range of 2–10 pixels (36–180 μm). For our initial calculations, however, we shall assume that all the blood vessels in the image are of equal width 2σ.

Now let us consider the detection of an arbitrary 1-D signal $s(t)$ in an additive Gaussian white noise. If the signal is passed through a filter with transfer function $H(f)$, the output signal $s_0(t)$ is given by

$$s_0(t) = \int H(f)\{S(f) + \eta(f)\} \exp(j2\pi ft)\, df \quad (1)$$

where $S(f)$ is the Fourier transform of $s(t)$, and $\eta(f)$ is the noise spectrum. Using Schwartz's inequality, it can be proved [29], [30] that the filter $H(f)$ that maximizes the output signal-to-noise ratio is given by $H_{opt}(f) = S^*(f)$. Since the input signal $s(t)$ is real valued, $h_{opt}(t) = s(-t)$. This optimal filter with the impulse response $h(t)$ is commonly known as the matched filter for the signal $s(t)$. In a typical communication system, if there are n different signals $s_i(t)$, $i = 1, 2, \cdots, n$, the received signal is passed through a stack of n matched filters. If the response due to the jth filter is the maximum, it is concluded that the signal $s_j(t)$ was transmitted.

Under the present context, it may be noted that the intensity profile can be assumed to be symmetrical about the straight line passing through the center of the vessel. Hence, $s(-t) = s(t)$. The optimal filter must have the same shape as the intensity profile itself. In other words, the optimal filter is given by $h_{opt}(d) = -\exp(-d^2/2\sigma^2)$. The negative sign indicates that the vessels are darker than the background. Also, note further that instead of n different types of objects having to be identified, the problem reduces to deciding whether or not a particular pixel belongs to a blood vessel. If the magnitude of the filtered output at a given pixel location exceeds a certain threshold, the pixel is labeled as a part of a vessel.

When the concept of matched filter is extended to two-dimensional images, it must be appreciated that a vessel may be oriented at any angle θ ($0 \le \theta \le \pi$). The matched filter $s(t)$ will have its peak response only when it is aligned at an angle $\theta \pm \pi/2$. Thus, the filter needs to be rotated for all possible angles, the corresponding responses are to be compared, and for each pixel only the maximum response is to be retained.

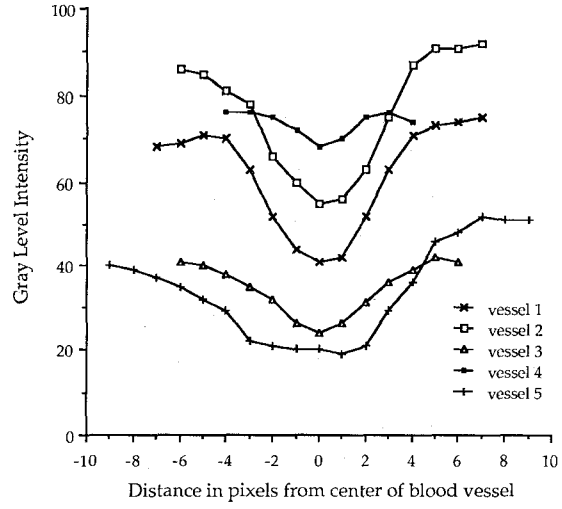

Fig. 1. The gray-level (brightness) profiles of the cross section of several blood vessels in the image of Fig. 7(a). The shapes of the curves are similar although the vessels have different widths and intensities. The trough in each curve represents the center of the corresponding blood vessel.

Consider the response of this filter for a pixel belonging to the background retina. Assuming the background to have constant intensity with zero mean additive Gaussian white noise, the expected value of the filter output should ideally be zero. The convolution kernel is, therefore, modified by subtracting the mean value of $s(t)$ from the function itself.

It has already been mentioned that the vessels may be considered as piecewise linear segments. Instead of matching a single intensity profile of the cross section of a vessel, a significant improvement can be achieved by matching a number of cross sections (of identical profile) along its length simultaneously. Such a kernel may be mathematically expressed as

$$K(x, y) = -\exp(-x^2/2\sigma^2) \quad \text{for } |y| \le L/2 \quad (2)$$

where L is the length of the segment for which the vessel is assumed to have a fixed orientation. Here the direction of the vessel is assumed to be aligned along the y-axis. For the vessels at different orientations, the kernel has to be rotated accordingly. L was determined experimentally by analyzing vessels in both normal and abnormal retinas. The above procedure reduces the possibility of false detection of blood vessels in a nonideal environment. Also, it suppresses the response due to the noise significantly in the background retina where no blood vessel is present. Such a scheme may be compared to Canny's edge detector [7], where the maximum of directional derivatives at every pixel is calculated and is averaged along its perpendicular direction.

IV. Implementation of the Algorithm

The two-dimensional matched filter kernel in a discrete grid is designed as follows. Let $\bar{p} = [x\ y]$ be a discrete

point in the kernel and θ_i be the orientation of the ith kernel matched to a vessel at an angle θ_i. In order to compute the weighting coefficients for the kernel, it is assumed to be centered about the origin [0 0]. The rotation matrix is given by

$$\bar{r}_i = \begin{bmatrix} \cos\theta_i & -\sin\theta_i \\ \sin\theta_i & \cos\theta_i \end{bmatrix}$$

and the corresponding point in the rotated coordinate system is given by $\bar{p}_i = [u\ v] = \bar{p}\,\bar{r}_i^T$. Assuming an angular resolution of 15°, we need 12 different kernels to span all possible orientations. A set of 12 such kernels is applied to a fundus image and at each pixel only the maximum of their responses is retained.

A Gaussian curve has infinitely long double sided trails. We truncate the trail at $u = \pm 3\sigma$. A neighborhood N is defined such that $N = \{(u, v) \mid |u| \leq 3\sigma, |v| \leq L/2\}$. The corresponding weights in the ith kernel are given by

$$K_i(x, y) = -\exp(-u^2/2\sigma^2) \quad \forall \bar{p}_i \in N. \tag{3}$$

If A denotes the number of points in N, the mean value of the kernel is determined as

$$m_i = \sum_{\bar{p}_i \in N} K_i(x, y)/A.$$

Thus, the convolutional mask used in this algorithm is given by $K_i'(x, y) = K_i(x, y) - m_i \ \forall \bar{p}_i \in N$.

Because of the hardware design of the image processing system, the weighting coefficients in the kernel need to be integers in the range (−128, 127). The coefficients are each multiplied by a scale factor of 10 and truncated to their nearest integer. A higher scale factor would increase the accuracy, but might lead to buffer overflow. Due to truncation errors, the mean value of the kernel may not be exactly equal to zero. Kernels, for which the mean value is positive, are forced to have slightly negative mean values in order to reduce the effect of background noise where no blood vessel is present. Two such kernels for two different angles are given in Fig. 2.

0	0	0	0	0	0	4	0	0	0	0	0	0	0	0	0
0	0	0	0	0	4	4	3	0	0	0	0	0	0	0	0
0	0	0	0	4	4	3	2	0	0	0	0	0	0	0	0
0	0	0	4	4	3	2	0	-2	-4	0	0	0	0	0	0
0	0	4	4	3	2	0	-2	-4	-5	-6	0	0	0	0	0
0	4	4	3	2	0	-2	-4	-5	-6	-5	-4	0	0	0	0
4	4	3	2	0	-2	-4	-5	-6	-5	-4	-2	0	0	0	0
0	3	2	0	-2	-4	-5	-6	-5	-4	-2	0	2	3	0	0
0	0	0	-2	-4	-5	-6	-5	-4	-2	0	2	3	4	4	0
0	0	0	-4	-5	-6	-5	-4	-2	0	2	3	4	4	0	0
0	0	0	0	-6	-5	-4	-2	0	2	3	4	4	0	0	0
0	0	0	0	0	-4	-2	0	2	3	4	4	0	0	0	0
0	0	0	0	0	0	0	2	3	4	4	0	0	0	0	0
0	0	0	0	0	0	0	3	4	4	0	0	0	0	0	0
0	0	0	0	0	0	0	0	4	0	0	0	0	0	0	0

(a)

0	0	0	0	0	0	0	0	0	0	0	0	0	0	0	0
0	0	0	0	0	0	0	0	0	0	0	0	0	0	0	0
0	0	0	0	0	0	0	0	0	0	0	0	0	0	0	0
0	4	3	2	1	-2	-5	-6	-5	-2	1	2	3	4	0	0
0	4	3	2	1	-2	-5	-6	-5	-2	1	2	3	4	0	0
0	4	3	2	1	-2	-5	-6	-5	-2	1	2	3	4	0	0
0	4	3	2	1	-2	-5	-6	-5	-2	1	2	3	4	0	0
0	4	3	2	1	-2	-5	-6	-5	-2	1	2	3	4	0	0
0	4	3	2	1	-2	-5	-6	-5	-2	1	2	3	3	0	0
0	4	3	2	1	-2	-5	-6	-5	-2	1	2	3	4	0	0
0	4	3	2	1	-2	-5	-6	-5	-2	1	2	3	4	0	0
0	4	3	2	1	-2	-5	-6	-5	-2	1	2	3	4	0	0
0	0	0	0	0	0	0	0	0	0	0	0	0	0	0	0
0	0	0	0	0	0	0	0	0	0	0	0	0	0	0	0
0	0	0	0	0	0	0	0	0	0	0	0	0	0	0	0

(b)

Fig. 2. Two of the 12 different kernels that have been used to detect vessel segments along different directions: (a) segments along the 45° direction; and (b) segments along the vertical direction. We have used $\sigma = 2.0$ and $L = 9$ to generate different kernels.

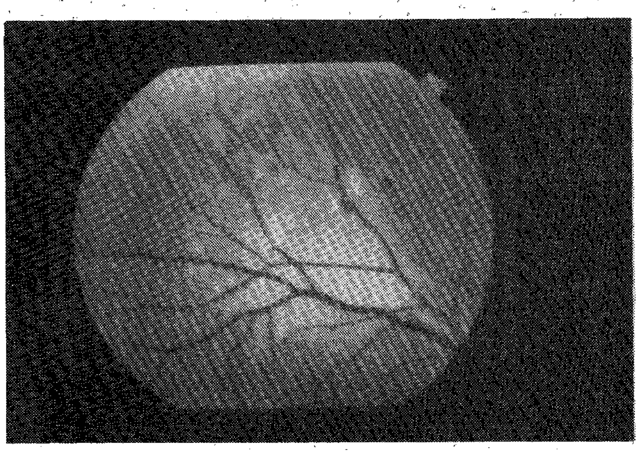

Fig. 3. A typical retinal image obtained from a fundus camera. The monochrome image represents the information contained in the green color plane only since this plane provides the highest vessel contrast.

Our system consists of a special image processing board from Matrox, Inc., known as the MVP-AT/NP, which is capable of computing the convolution of sizes up to 32 × 32 for an image of size 512 × 480 in a few hundred milliseconds. The software runs on a Compaq 386 and the execution time for this algorithm is about 50 s, including the rotation of the kernel for 12 different directions. The images are digitized from 35 mm transparencies taken from a TOPCON TRV-50 fundus camera at 35° field of view.

V. Results and Discussions

An original fundus image is given in Fig. 3, and the result of the application of this filter is given in Fig. 4. For this case, we choose $\sigma = 2$ and $L = 9$. The original image was smoothed by a 5 × 5 mean filter to reduce the effect of spurious noise. The Sobel operator and the morphological edge detector [3] were also applied to the same image, and the corresponding filtered images are given in Figs. 5 and 6, respectively. Comparing these three filtered images, we may conclude that the given algorithm achieves significant improvement compared to other algorithms in detecting blood vessels. For the purpose of comparison, the original gray-scale output images were used.

Fig. 7(a) represents another fundus image, and Fig. 7(b), (c), and (d) are the results of applying the Sobel operator, the morphological edge detector, and the proposed algorithm, respectively. It may be noticed here that, unlike Sobel or morphological operators where only the edges are detected, the proposed algorithm extracts the blood vessel as a whole. The "anti-parallels" are de-

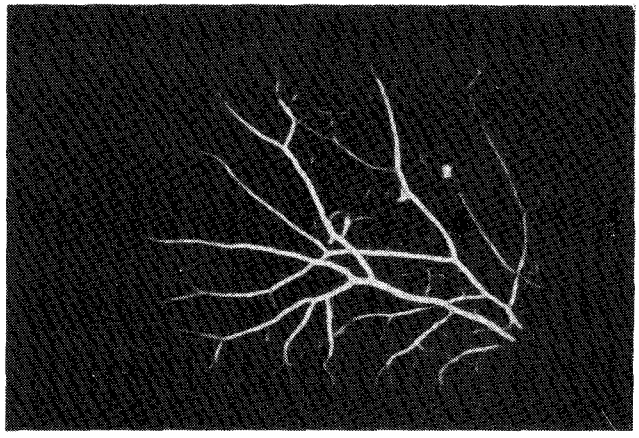

Fig. 4. The result of application of the matched filter to the image given in Fig. 3. The edges at the image border due to the aperture of the fundus camera have been removed by fitting an ellipse around the image. The output images shown in this paper represent the gray-scale response of the filters.

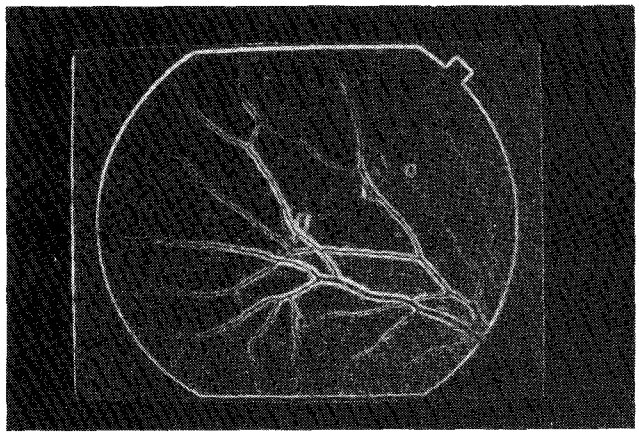

Fig. 5. Edge detection is performed on the image given in Fig. 3 using the Sobel operator.

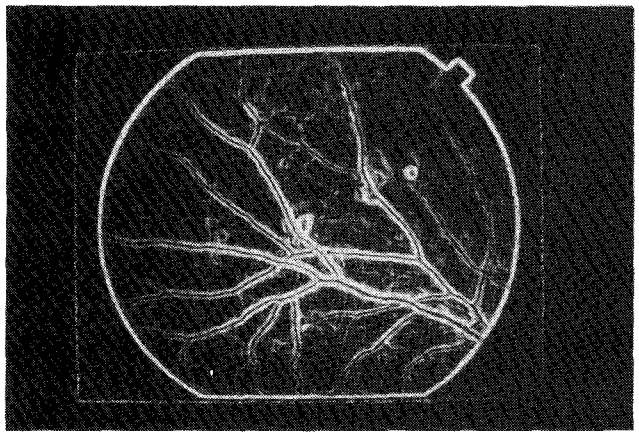

Fig. 6. The result of application of the morphological edge detector to the image in Fig. 3.

tected from the edge detected image in Fig. 7(b) and are tracked along the gradient direction (refer to [22]) to extract the blood vessel segments. The result is given in Fig. 8. When the results in Figs. 7(d) and 8 are compared, it is readily seen that the proposed algorithm preserves the continuity of the vessels in the image. Also, we have found the algorithm to perform effectively in detecting blood vessels even when the local contrast is quite low.

Careful observation of results in Figs. 4 and 7(d) would reveal that we, indeed, get some response due to edges of other bright objects (such as lesions, optic disk, etc.) which do not resemble any vessel segment. This is due to the fact that the local contrast is very high and the edges of the objects partially match the shape of the kernel. Such edges also appear when other methods are used. A post-processing step is needed to identify and subsequently eliminate such false detection.

Some vessels may have a specular bright reflex running through their center [31]. This could be due to certain pathological conditions of the patient or due to the nature of illumination. However, we found such a "bump" at the center of the intensity profile to be quite small compared to the brightness of its neighborhood. The effect of such a reflex on the results of the matched filter were, therefore, negligible.

It was mentioned earlier that the parameter L was chosen to be equal to 9 pixels which correspond to about 160 μm. Ideally, one would like to have a larger value of L which would further reduce the noise. However, the resulting template might not match well if the vessels were quite tortuous in nature (as in central retinal vein occlusions). $L = 9$ at the working level of magnification was experimentally found to be a good choice as it performs well even for detecting tortuous vessel segments.

Twelve different templates were used in the proposed scheme to search for directional components along all possible orientations, since vessel segments lying within $\pm 7.5°$ of the direction of the chosen kernel were found to respond well. The performance of the proposed scheme with 24 templates, using integer valued kernels, was virtually indistinguishable from that of 12 templates. Higher precision can be achieved by performing convolutions in floating point hardware or software, with a sacrifice in speed. A fewer number of templates may be used to obtain faster results, however, at least 4–6 such templates are needed to have a reasonably good enhancement of vessel segments.

Applications of the above designed filters enhance individual vessel segments in the image. A proper thresholding scheme can be used to distinguish between enhanced vessel segments and the background. An automatic thresholding algorithm that maximizes the inter-class intensity variance [32] was used to binarize the enhanced images.

Convolution with a Gaussian window does not displace the second-order zero-crossings of the original intensity data. Thus, the detected blood vessels have good edge localization. This convolution process also eliminates the noise outside the desired frequency band [4].

We initially assumed that the blood vessels are of uniform caliber. One way of accommodating the varying vessel widths in the proposed scheme is to run the pro-

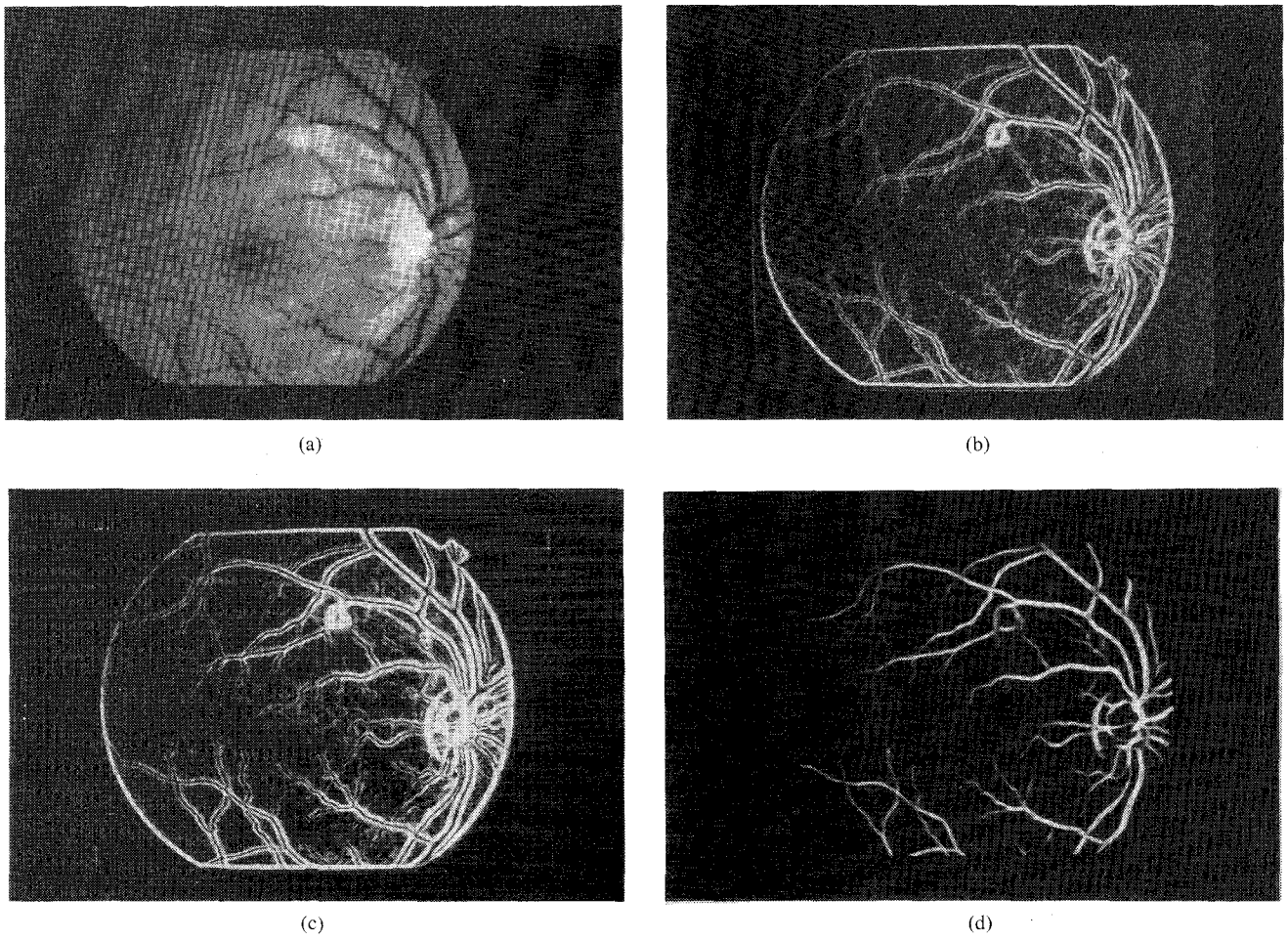

(a) (b) (c) (d)

Fig. 7. Three different filters are applied to a different fundus image: (a) the original image; (b) edge detection by using Sobel operator; (c) edge detection by using morphological edge detector; and (d) detection of blood vessels by using the proposed 2-D matched filter.

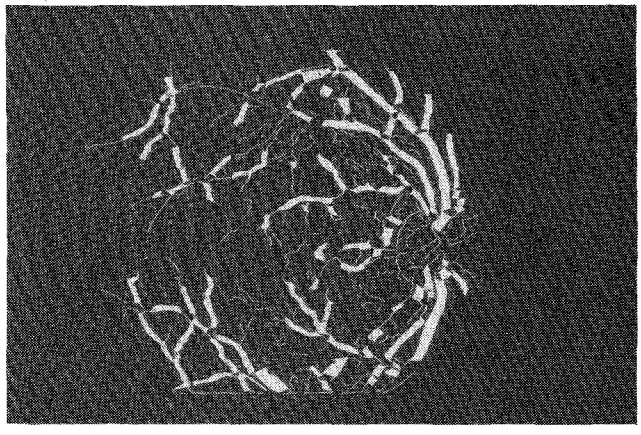

Fig. 8. The edges from Fig. 7(b) are tracked as shown here by the continuous lines. The "anti-parallels" are then detected and filled in to identify blood vessel segments. The results show that the detected blood vessels are broken into several segments due to the vessel branchings and crossings.

gram with kernels having different values of σ. Here the computation increases linearly with the number of different widths being considered. However, practical experimentations suggest that the amount of improvement achieved does not warrant such extra computations. We have used $\sigma = 2$, which matched well with a blood vessel of medium caliber for the retinal images being considered with our apparatus. Nonetheless, from Figs. 4 and 7(d), it is clear that vessels from maximum diameter down to nearly capillary size also responded well to the chosen value of σ.

Lastly, it may be commented here that the matched filter detection method is applicable only to stationary processes. Usually, a pre-processing step is performed in which the local mean is subtracted from the image and then the pixel intensities are divided by the square root of the local variances to approximate the image as a stationary process. This pre-processing step may be omitted as the qualitative improvement is almost insignificant.

VI. Conclusions

We have introduced a simple operator for feature detection based on the optical and spatial properties of objects (namely blood vessels) to be recognized. The proposed scheme retains the computational simplicity of the enhancement/thresholding type of edge operators, and at the same time incorporates the advantages of using model-

based edge detectors. Because of the large size of the convolutional kernel, it may take a long time to run this algorithm on an ordinary computer. However, these operators can be efficiently implemented in many machine vision systems having special hardware support for real time convolution operations.

This method performs well in analyzing fluorescein angiogram images of the retina as well. With minor modifications, this method could very well be extended to the extraction of geological features from satellite images and the enhancement of fingerprint images.

Acknowledgment

The authors would like to thank T. Clark for his help in obtaining the images used in this research. The suggestions and comments by anonymous reviewers are also gratefully acknowledged.

References

[1] I. E. Abdou and W. K. Pratt, "Quantitative design and evaluation of enhancement/thresholding edge detectors," *Proc. IEEE*, vol. 67, pp. 753-763, May 1979.

[2] W. K. Pratt, *Digital Image Processing*. New York: Wiley, 1978.

[3] R. M. Haralick, J. S. J. Lee, and L. G. Shapiro, "Morphological edge detection," *IEEE J. Robotics Automat.*, vol. RA-3, pp. 142-155, Apr. 1987.

[4] D. Marr and E. Hildreth, "Theory of edge detection," *Proc. Roy. Soc. London, Ser. B*, vol. 207, pp. 187-217, 1980.

[5] D. Talton, "Implementation of a Gaussian-smoothed gradient-edge operator," Dep. Elec. Eng., Univ. Pennsylvania, Tech. Rep. MS-CIS-85-12, 1985.

[6] T. Elfving, J.-O. Eklundh, and S. Nyberg, "Edge detection using the Marr-Hildreth operator with different sizes," in *Int. Conf. on Pattern Recognition*, 1982, pp. 1109-1112.

[7] J. Canny, "A computational approach to edge detection," *IEEE Trans. Pattern Anal. Machine Intell.*, vol. PAMI-8, pp. 679-697, Nov. 1986.

[8] V. Torre and T. A. Poggio, "On edge detection," *IEEE Trans. Pattern Anal. Machine Intell.*, vol. PAMI-8, pp. 147-163, Mar. 1986.

[9] M. H. Hueckel, "An operator which locates edges in digitized pictures," *J. Ass. Comput. Mach.*, vol. 18, pp. 113-125, Jan. 1971.

[10] ——, "A local operator which recognizes edges and lines," *J. Ass. Comput. Mach.*, vol. 20, pp. 634-647, Oct. 1973.

[11] F. O'Gorman, "Edge detection using Walsh functions," *Artificial Intell.*, vol. 10, pp. 215-223, 1978.

[12] W. Frei and C. C. Chen, "Fast boundary detection: A generalization and a new algorithm," *IEEE Trans. Comput.*, Oct. 1977.

[13] F. M. Dickey, K. S. Shanmugam, and J. A. Green, "An optimal frequency domain filter for edge detection in digital pictures," *IEEE Trans. Pattern Anal. Machine Intell.*, vol. PAMI-1, pp. 37-49, Jan. 1979.

[14] J. W. Modestino and R. W. Fries, "Edge detection in noisy images using recursive digital filtering," *Comput. Graphics Image Processing*, vol. 6, pp. 409-433, 1977.

[15] T. H. Laffey, L. T. Watson, and R. M. Haralick, "Topographic classification of digital image intensity surfaces using generalized splines and the discrete cosine transformation," *Comput. Vision, Graphics, Image Processing*, vol. 29, pp. 143-167, 1985.

[16] L. D. Andrews and S. Sinclair, "Macro-vascular topography in diabetic retinopathy: Analysis of fundus pictures using high resolution digital image processing," in *ARVO Abstract*, p. 262, 1988.

[17] M. Tanaka and K. Tanaka, "An automatic technique for fundus-photograph mosaic and vascular net reconstruction," in *MEDINFO '80*. Amsterdam, The Netherlands: North-Holland, 1980, pp. 116-120.

[18] Y. Okamoto, S. Tamura, and K. Yanashima, "Zero-crossing interval correction in tracing eye-fundus blood vessels," *Pattern Recognition*, vol. 21, pp. 227-233, 1988.

[19] S. Yamamoto and H. Yokouchi, "Automatic recognition of color fundus photographs," in *Digital Processing of Biomedical Images*. New York: Plenum, 1976, pp. 385-397.

[20] K. Akita and H. Kuga, "Digital processing of color ocular fundus images," in *MEDINFO '80*. Amsterdam, The Netherlands: North-Holland, 1980, pp. 80-84.

[21] K. Akita and H. Kuga, "Pattern recognition of blood vessel networks in ocular fundus images," in *IEEE Int. Workshop Phys. and Eng. in Med. Imaging*, Mar. 15-18, 1982, pp. 436-441.

[22] R. Nevatia and K. R. Babu, "Linear feature extraction and description," *Comput. Graphics Image Processing*, vol. 13, pp. 257-269, 1980.

[23] M. Nelson N. Katz, M. Goldbaum, and S. Chaudhuri, "An image processing system for automatic retina diagnosis," in *Proc. SPIE Conf. Elec. Imaging, Devices and Syst.*, Los Angeles, CA, Jan. 10-14, 1988, vol. 902.

[24] E. Peli, "Adaptive enhancement based on visual model," *Opt. Eng.*, vol. 26, pp. 655-660, July 1987.

[25] R. M. Rangayyan, S. Walsh, S. Chaudhuri, H. Nguyen, and C. B. Frank, "A Fourier domain directional filtering method for analysis of collagen alignment in ligaments," *IEEE Trans. Biomed. Eng.*, vol. BME-34, pp. 509-518, July 1987.

[26] S. Chaudhuri, "Digital image processing techniques for quantitative analysis of collagen fibril alignment in ligaments," M.S. thesis, Univ. Calgary, 1987.

[27] L. O'Gorman and J. V. Nickerson, "Matched filter design for fingerprint image enhancement," in *IEEE Int. Conf. Acoust., Speech, and Signal Processing*, New York, 1988, pp. 916-919.

[28] L. O'Gorman and J. V. Nickerson, "An approach to fingerprint filter design," *Pattern Recognition*, vol. 22, pp. 29-38, Jan. 1989.

[29] S. Haykin, *Communication Systems*. New Delhi: Wiley Eastern, 1979.

[30] D. H. Friedman, *Detection of Signals by Template Matching*. Baltimore, MD: Johns Hopkins University Press, 1969.

[31] F. C. Delori, "Noninvasive technique for oximetry of blood in retinal vessels," *Appl. Opt.*, vol. 27, pp. 1113-1125, Mar. 1988.

[32] N. Otsu, "A threshold selection method from gray-level histograms," *IEEE Trans. Syst., Man, Cybern.*, vol. SMC-9, pp. 62-66, Jan. 1979.